An Investigation of the Dark Formation of Nitrous Acid in Environmental Chambers

JAMES N. PITTS, JR.,* EUGENIO SANHUEZA,†
ROGER ATKINSON, WILLIAM P. L. CARTER,
ARTHUR M. WINER, GEOFFREY W. HARRIS,‡
and CHRISTOPHER N. PLUM¶

Abstract

The formation of nitrous acid (HONO) in the dark from initial concentrations of NO_2 of 0.1–20 ppm in air, and the concurrent disappearance of NO_2, were monitored quantitatively by UV differential optical absorption spectroscopy in two different environmental chambers of ca.4300- and 5800-L volume (both with surface/volume ratios of 3.4 m^{-1}). In these environmental chambers the initial HONO formation rate was first order in the NO_2 concentration and increased with the water vapor concentration. However, the HONO formation rate was independent of the NO concentration and relatively insensitive to temperature. The initial pseudo-first-order consumption rate of NO_2 was $(2.8 \pm 1.2) \times 10^{-4}$ min^{-1} in the 5800-L Teflon-coated evacuable chamber and $(1.6 \pm 0.5) \times 10^{-4}$ min^{-1} in a 4300-L all-Teflon reaction chamber at ca.300 K and ca.50% RH. The initial HONO yields were ca.40–50% of the NO_2 reacted in the evacuable chamber and ca.10–30% in the all-Teflon chamber. Nitric oxide formation was observed during the later stages of the reaction in the evacuable chamber, but ca.50% of the nitrogen could not be accounted for, and gas phase HNO_3 was not detected. The implications of these data concerning radical sources in environmental chamber irradiations of NO_x-organic-air mixtures, and of HONO formation in polluted atmospheres, are discussed.

Introduction

The photolysis of nitrous acid (HONO) in the actinic UV region [1]

$$(1) \qquad HONO + h\nu \ (\lambda \sim 290\text{--}400 \ nm) \rightarrow OH + NO$$

is an important process in urban atmospheres and in smog chamber irradiations since it produces the OH radical, a key participant in the

formation of photochemical smog [2–4]. During daylight hours or during environmental chamber irradiations, HONO is formed largely by the reaction of OH radicals with NO [5].

$$\text{(2)} \qquad\qquad OH + NO \xrightarrow{M} HONO$$

This reaction, when balanced by its rapid photolysis via reaction (1), leads to a steady-state concentration of HONO and no net production of OH radicals. However, if HONO is also formed by some nonphotolytic, nonradical reaction, then its subsequent rapid photolysis would represent a net source of OH radicals both in the atmosphere during the period around sunrise [4] and during the initial stages of environmental chamber irradiations [6,7].

Recently we have used long path (0.8–2.3 km) UV differential optical absorption spectroscopy (DOAS) to show that HONO can accumulate up to levels of ca.8 ppb at night in urban areas such as Los Angeles [4,8] and can remain at levels above 6 ppb for as long as 5 h [4]. However, it is not known at the present time to what extent this nighttime increase in HONO is due to its homogeneous [9] or heterogeneous formation from NO_2 (or other nitrogenous compounds) present in the atmosphere, direct emissions from automobiles [10], or some combination of these processes.

In environmental chamber systems, HONO photolysis is believed to contribute, at least in part, to the excess rate of formation of radicals characteristic of those systems [6,7], which complicates the use of environmental chamber data for testing computer kinetic models of photochemical smog formation [11]. In particular, in a series of environmental chamber experiments designed to measure OH radical levels in NO_x-air irradiations, we observed an initial, rapidly-decaying radical source [6,7]. This was almost certainly due to the photolysis of initially present HONO, since direct *in situ* spectroscopic measurements of HONO using the DOAS technique agreed well with values calculated to fit the observed OH radical concentration-time profiles [7].

The initial presence of HONO in our environmental chamber experiments was not unexpected, since it had previously been observed to be formed from high concentrations of NO and NO_2 in humid air [12,13]. However, the amount of HONO formed prior to irradiation in our 5800-L evacuable chamber appeared to increase with the NO_2 concentration, the relative humidity and the temperature, but be independent of (or indeed decrease with) the initial NO concentration [7]. These observations showed that the heterogeneous reaction

$$\text{(3)} \qquad\qquad NO + NO_2 + H_2O \xrightarrow{\text{wall}} 2\,HONO$$
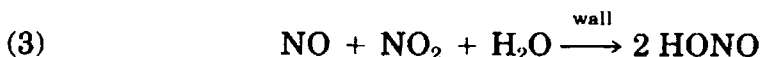
could not be responsible for this observed formation of HONO under these conditions, but suggested that a reaction of NO_2 with water was occurring [7].

$$(4) \qquad 2\,NO_2 + H_2O \xrightarrow{\text{wall}} HONO + HNO_3$$
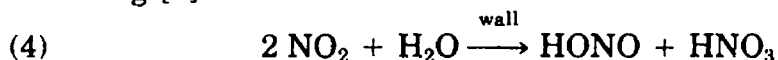
In any case, the photolysis of initially present HONO cannot be the entire radical source, since a continuous chamber radical source was also observed throughout NO_x-air irradiations, long after any initially present HONO was removed by photolysis [7]. If the photolysis of HONO is also the cause of this chamber radical source, the HONO must be continuously formed during the irradiation by a process other than reaction (2).

Recently, Sakamaki, Hatakeyama, and Akimoto [14] have also observed that HONO is formed in the dark from NO_2, at initial concentrations of ca.1–20 ppm in air, in a 6065-L Teflon-coated environmental chamber at a rate which could contribute, at least in part, to the continuous radical source we had earlier observed in NO_x-air irradiations. Their data also showed that the observed HONO did not result from reaction (3). This observation is consistent with previous studies of this reaction which showed it to be too slow to be of importance in the part-per-million (ppm) concentration regime of interest here [12,13,15]. Rather, Sakamaki, Hatakeyama, and Akimoto [14] attributed the formation of HONO to the heterogeneous hydrolysis of NO_2, which they wrote as the nonstoichiometric reaction (4').

$$(4') \qquad NO_2 + H_2O \xrightarrow{\text{wall}} \rightarrow HONO$$
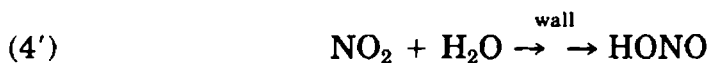
Interestingly, gas phase HNO_3 was not observed, although nitric oxide was formed at an ca.10% yield [14].

Previous studies of the hydrolysis of NO_2 were conducted at higher surface/volume (S/V) ratios, and differ on the rate of reaction and reaction order in NO_2. Thus England and Corcoran [16] studied the NO_2-H_2O system at NO_2 concentrations from 15.5–46.5 ppm and water vapor concentration $\leqslant 1.5 \times 10^4$ ppm (40% relative humidity). They observed that the initial rate of disappearance of NO_2 was first order with respect to the water vapor concentration but was greater than first order with respect to NO_2. They also determined, by use of two Pyrex reactors with S/V ratios of 35.5 and 120 m^{-1}, that the rate of reaction was independent of the S/V ratio. Nitric oxide was the only product actually detected, at concentrations corresponding to ca.30% of the NO_2 consumed.

More recently Lee and Schwartz [17] studied the reaction of gaseous NO_2 with liquid water at low NO_2 partial pressures. The observed products were equal amounts of nitrite and nitrate. At a steady-state

aqueous phase concentration of NO_2 the rate of reaction was observed to be second order with respect to the NO_2 pressure [17].

We report here results of an extensive series of measurements of HONO formation from NO_2 at concentrations down to ca.100 ppb, levels commonly observed in urban atmospheres. These experiments were conducted in the dark in two different environmental chambers, employing the sensitive, *in situ*, DOAS technique to concurrently monitor ppb levels of HONO and NO_2. These results lead to a better understanding of the characteristics and range of variability of this important process in environmental chambers, and its relevance to polluted ambient atmospheres.

Experimental

The majority of the experiments were carried out in the SAPRC 5800-L evacuable, thermostatted, environmental chamber (EC) [18]. This cylindrical chamber is Teflon-coated with quartz end-windows mounted in a Teflon-coated aluminum grid [18]. It has a diameter of 1.37 m and a length of 3.96 m, yielding a S/V ratio of 3.4 m^{-1}, with the window surfaces contributing ca.18% of the total surface area. Experiments were carried out at temperatures ranging from 283–323 K at a relative humidity (RH) of 50%, although several experiments were carried out at lower and higher RH. Initial NO and NO_2 levels ranged from 0 to ca.20 ppm.

Between experiments the chamber was evacuated for several hours (generally overnight) to $\leqslant 2 \times 10^{-5}$ torr. The chamber was then filled with pure air [18,19] of the desired humidity (determined by wet bulb/dry bulb measurements) to approximately 730-torr total pressure, and then NO_2 and NO (if any) were flushed by a stream of ultrahigh purity nitrogen into the chamber from a ca.5-L bulb attached to a vacuum gas-handling line. The NO was purified by passage through a trap containing activated Linde Molecular Sieve 13X, and NO_2 was prepared by reaction of this purified NO with 1 atm of ultrahigh purity O_2, which had also been passed over 13X Molecular Sieve. The contents of the chamber were mixed with two stirring fans for a minimum of five minutes after addition of NO and NO_2, and the chamber was maintained at the desired temperature by means of the chamber's heating/cooling system [18].

Nitrous acid and NO_2 were monitored by DOAS using a multiple pass White-type optical system (3.77-m base path) arranged along the longitudinal axis of the chamber. A 75-W Xe light source was focused by a spherical mirror to match the focal length of the multiple pass optical system. Forty passes through the chamber, and thus a 150.8-m

total path length, were used, leading to a sensitivity of ca.5 ppb for HONO and ca.20 ppb for NO_2.

After transmission through the chamber, the beam was focused on the entrance slit of a 0.3-m McPherson spectrograph equipped with a 600 groove mm^{-1} grating (dispersion ca.4 nm mm^{-1}). A thin metal disc (20-cm diameter), rotating at 1.1 Hz, with 100 radial slits (100-μm wide, ca.16-mm spacing) was placed in the exit focal plane. The light intensity passing through a slit was monitored by a photomultiplier (EMI 9659Q), and the signal in each of 350 channels measured for ca.20 μs. The signals were then digitalized (12 bits) and stored by a computer (DEC MINC-11/23) to average the scans and to permit spectral deconvolution and calculation of optical densities. With this arrangement a 40-nm segment of the dispersed spectrum was scanned repetitively in any specific spectral region. In these studies the near-UV region from ca.335 to 375 nm was utilized since the absorption spectra of HONO and NO_2 both show distinct structure in this wavelength range.

A more limited set of experiments was carried out in a ca.4300-L indoor all-Teflon (FEP, 2 mil thickness) chamber (ATC) also equipped with an *in situ*, multiple pass optical system interfaced to a monochromator-photomultiplier combination for DOAS. The base path of this optical system was 2.15 m, corresponding to a total path length of 102.5 m for 48 passes. The operating conditions and techniques used were essentially identical to those described above for the 5800-L evacuable chamber. The S/V of 3.4 m^{-1} for this chamber was identical to that for the 5800-L evacuable chamber.

In addition to measurements of HONO and NO_2 by DOAS, NO and (NO_x-NO) were measured directly after the injection with a commercial chemiluminescence NO-NO_x analyzer (TECO Model 14B). For selected runs NO was monitored with a SAPRC-built chemiluminescence NO monitor which had a detection sensitivity of ca.1 ppb. In one evacuable chamber run (EC-784) a search was made for gas phase HNO_3 by long path Fourier transform infrared (FTIR) absorption spectroscopy using a pathlength of 80 m. The HNO_3 detection limit for this technique was ca.40 ppb under the conditions employed.

Results

Evacuable Chamber Studies

As noted above, the majority of the environmental chamber experiments were conducted in the SAPRC 5800-L Teflon-coated environmental chamber. Two series of experiments, separated by over a year,

were conducted in that chamber, and the conditions and results of these experiments are summarized in Table I.

In all cases HONO formation was observed, together with a disappearance of NO_2, as shown, for example, in Figure 1 for run EC-758. In order to assess whether background offgassing of HONO could be a contributing factor, one experiment (EC-778) was carried out with the evacuable chamber filled with pure air alone at 50% RH and 297 K. The HONO, NO, and NO_2 offgassing rates were measured and observed to be 0.001 ± 0.0003, 0.002 ± 0.0004, and 0.004 ± 0.001 ppb min $^{-1}$, respectively. These were generally minor compared to the observed formation or decay rates (Table I), indicating that the presence of NO_2 is required for any significant HONO formation to occur.

For many of the experiments, data were obtained over reaction periods of up to 2–3 days. In the case of run EC-758, data were obtained over a period of ca.21 h and as seen in Figure 1 the HONO formation rate and the NO_2 disappearance rate both decreased with the reaction time (with the former generally decreasing faster than the latter). However, within the experimental errors, the HONO formation rates and the NO_2 disappearance rates were constant for up to 2–3 h for initial NO_2 concentrations ⩾350 ppb, and up to ca.24 h for experiments with initial NO_2 concentrations of ⩽100 ppb. Table I also gives these initial HONO formation and NO_2 disappearance rates.

The data in Table I and Figure 1 show that during the initial stages of the experiments the stoichiometry (Δ[HONO]/-Δ[NO_2]) is close to, though generally somewhat less than, 0.5. However, at extended reaction times the ratio (Δ[HONO]/-Δ[NO_2]) typically decreased, as shown by the data in Table I. While NO was also identified during these runs, significant amounts were only observed after a rather long induction period. For runs where NO was monitored Table I gives the NO and HONO yields observed at the termination of the runs, together with the final amount of NO_2 consumed. It can be seen from this table that the observed NO and HONO yields account for only ca. 50% of the NO_2 reacted.

The rate of HONO formation in the evacuable chamber depended to a certain extent on the previous history of the chamber. While runs with the chamber "unconditioned" (i.e., pumped for ⩽1 h) gave lower HONO production rates than for runs where the chamber had been pumped for ⩾1 h, the HONO formation rate was significantly higher after the chamber was cleaned by the irradiation of ca.1 torr of Cl_2 in 10 torr of N_2, followed by an overnight evacuation at ca.360 K (see EC-765 in Table I). The HONO formation rate subsequently returned to more typical values (see EC-774 and following runs) after the chamber

TABLE I. Conditions and selected results of the NO_x-H_2O-air experiments conducted in the SAPRC evacuable chamber.

EC Run Number	Initial [NO$_2$] (ppb)	Initial [NO] (ppb)	Temperature (K)	RH (%)	Initial d[HONO]/dt (ppb min^{-1})	Initial $-$d[NO$_2$]/dt (ppb min^{-1})	Initial $\frac{d[HONO]/dt}{-d[NO_2]/dt}$	Final t (min)	Final Δ[NO$_2$] (ppb)	Final Yield/Δ[NO$_2$] HONO	NO	N-loss[a]
558	190	0	305	50	0.032 ± 0.002	0.078 ± 0.007	0.42	204	15	0.43	0	0.57
545	354	93	305	50	0.069 ± 0.004	–	–					
546	360	920	305	50	0.048 ± 0.003	–						
557	380	0	305	50	0.060 ± 0.003	–	–					
556	383	0	305	50	0.037 ± 0.004	0.10 ± 0.01	0.37	270	21	0.48	–	–
544	400	0	305	50	0.064 ± 0.004	–	–					
564	590	187	305	50	0.068 ± 0.006	–						
555	733	0	305	50	0.100 ± 0.005	0.21 ± 0.06	0.48	120	25	0.48	0	0.52
548	878	900	305	50	0.15 ± 0.007	–	–					
559	1563	0	305	50	0.13 ± 0.007	–	–					
560	1682	0	305	50	0.13 ± 0.006	–	–					
549	1750	900	305	50	0.15 ± 0.008	–	–					
547	400	0	305	3	0.030 ± 0.006	–	–					
554	353	978	305	16	0.039 ± 0.003	–	–					
566	610	215	305	35	0.049 ± 0.005	–	–					
565	600	130	305	65	0.150 ± 0.02	–	–					
563	751	0	305	65	0.21 ± 0.006	–	–					

TABLE I. *(continued from previous page)*

EC Run Number	Initial [NO$_2$] (ppb)	Initial [NO] (ppb)	Temperature (K)	RH (%)	Initial d[HONO]/dt (ppb min^{-1})	Initial $-$d[NO$_2$]/dt (ppb min^{-1})	$\dfrac{\text{d[HONO]/dt}}{-\text{d[NO}_2\text{]/dt}}$	Final t (min)	Final Δ[NO$_2$] (ppb)	Yield/Δ[NO$_2$] HONO	Yield/Δ[NO$_2$] NO	Yield/Δ[NO$_2$] N-loss[a]
778[b]	0	0	297	50	0.001 ± 0.0003	−0.004 ± 0.001	−	−	−	−	−	−
781	58	0	297	50	0.004 ± 0.001[c]	0.009 ± 0.002[c]	0.44	2565	27	0.26	0.19	0.55
780	100	100	297	50	0.010 ± 0.002[c]	−	−	−	−	−	−	−
779	112	0	297	50	0.012 ± 0.002[c]	0.025 ± 0.004[c]	0.48	1550	31	0.42	0.16	0.42
782	160	0	297	50	0.013 ± 0.001	0.027 ± 0.005	0.48	1850	51	0.35	−	−
759	281	0	297	50	0.031 ± 0.004	−	−	1455	103	0.39	−	−
763	354	0	297	50	0.058 ± 0.005	0.103 ± 0.017	0.56	390	40	0.56		
764	364	~1000	297	50	0.052 ± 0.006	−	−	−	−	−	−	−
757	530	0	297	50	0.061 ± 0.005	0.13 ± 0.03	0.47	285	37	0.47	−	−
765[d]	544	0	297	50	0.123 ± 0.009	0.334 ± 0.015	0.37	1360	250	0.26	−	−
775	550	0	297	50	0.056 ± 0.006	−	−	−	−	−	−	−
753	580	0	297	50	0.069 ± 0.004	0.169 ± 0.013	0.41	360	61	0.41		
774C[e]	763	0	297	50	0.075 ± 0.005	0.193 ± 0.014	0.39	−	−	−	−	−
758	840	0	297	50	0.107 ± 0.007	0.28 ± 0.06	0.38	1315	261	0.31	−	−
754	1080	0	297	50	0.095 ± 0.006	0.28 ± 0.05	0.34	1400	300	0.25		
774A	1529	0	297	50	0.207 ± 0.013	0.44 ± 0.08	0.47	1500	435	0.32	0.23	0.45

761	2242	0	297	50	0.10 ± 0.07	0.19 ± 0.05	0.53	1470	428	0.26	–	–
783	5000	0	297	50	0.229 ± 0.012	–	–	–	–	–	–	–
784	20000	0	297	50	0.806 ± 0.013	–	–	–	–	–	–	–
776	685	0	297	5	0.012 ± 0.004	–	–	1400	85	0.27	0.12	0.60
760	543	0	297	22	0.025 ± 0.006	–	–	1500	112	0.31	–	–
552	340	917	283	50	0.026 ± 0.003	–	–	–	–	–	–	–
553	375	990	323	16	0.040 ± 0.003	–	–	–	–	–	–	–

[a] N loss = $(\Delta[NO_2]-[HONO]-[NO])/\Delta[NO_2]$. Presumed to be due to formation of HNO_3 on the walls (see discussion).
[b] Chamber offgassing rate, $d[NO]/dt$ = 0.002 ± 0.0004 ppb min^{-1} (Δt = 71 h).
[c] Values corrected by chamber offgassing rates.
[d] Run performed after cleaning the chamber (see text).
[e] Run performed after the HONO photolysis of run 774A.
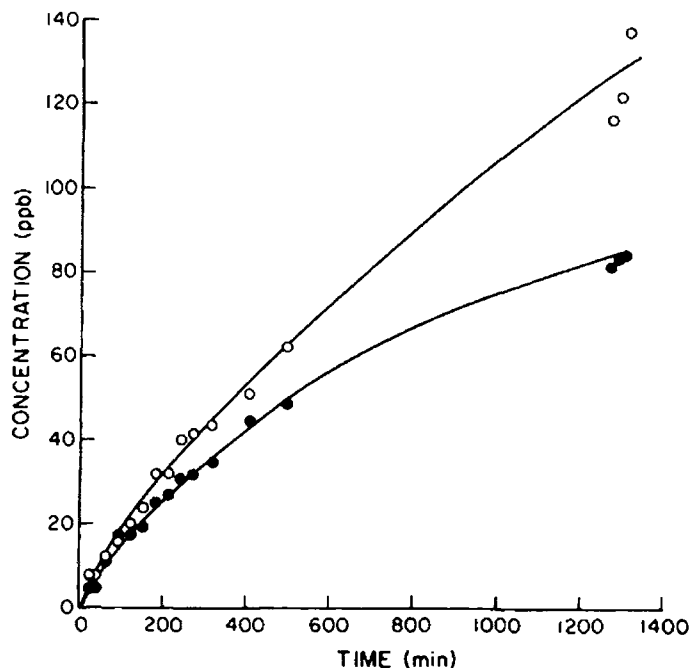[f] HONO measured by FTIR:$[HNO_3]$ <40 ppb for [HONO] = 387 ppb.

Figure 1. Plots of HONO formation and the observed amount of NO_2 consumed for run EC-758. (O) 0.5 × $-\Delta NO_2$, (●) HONO.

had been conditioned by a series of NO_x-air and propene-NO_x-air irradiations. In order to obtain reproducible results the chamber needed to be evacuated to $\leqslant 2 \times 10^{-5}$ torr for several hours prior to an experiment, and occasional 1-h irradiations of the evacuated chamber using the 25-KW solar simulator also appeared to help in the conditioning process. Except as noted, all runs reported in Table I were carried out after the chamber had been suitably conditioned.

The initial HONO formation rates, $(d[\text{HONO}]/dt)_{\text{init}}$, at ca.50% RH and 297 and 305 K (the conditions at which the majority of the experiments were carried out) are plotted against the NO_2 concentration in Figure 2. It can be seen that the sets of data obtained at 305 K and 50% RH and at 297 K and 50% RH (sets of runs which were carried out more than a year apart) are, within the scatter of the data, essentially indistinguishable. This shows that, after suitable conditioning, the reaction forming HONO is reasonably reproducible in this particular chamber.

Figure 2 also shows that for the evacuable chamber, at a constant temperature and relative humidity, the plot of ln $(d[\text{HONO}]/dt)_{\text{init}}$ against ln $[NO_2]$ is, with the scatter of the data, essentially linear with a slope close to unity. This implies that the initial HONO formation rate is approximately first order in NO_2. It is also evident from the data obtained at 287 and 305 K and ca.50% RH (Table I and Figure

2) that within the scatter of the data the HONO formation rate was independent of the initial NO concentration.

Since at a given temperature and water vapor concentration the initial HONO formation rate is linearly dependent on the initial NO_2 concentration, the quantity $\{(d[HONO]/dt)/[NO_2]\}_{init}$ defines an "effective" first-order rate constant which may be a function of temperature and water vapor concentration. The dependence of $\{(d[HONO]/dt)/[NO_2]\}_{init}$ on the water vapor concentration at 305 and 297 K is shown in Figure 3, which also shows the values of $\{(d[HONO]/dt)/[NO_2]\}_{init}$ at the other temperatures and water concentrations studied. The ratio $\{(d[HONO]/dt)/[NO_2]\}_{init}$ increases with the water vapor concentration, though the scatter of the data does not allow a conclusion to be drawn as to whether this dependence is linear or not. Additionally, as shown in Figure 3, the scatter of the data do not allow any conclusions to be drawn concerning the effects
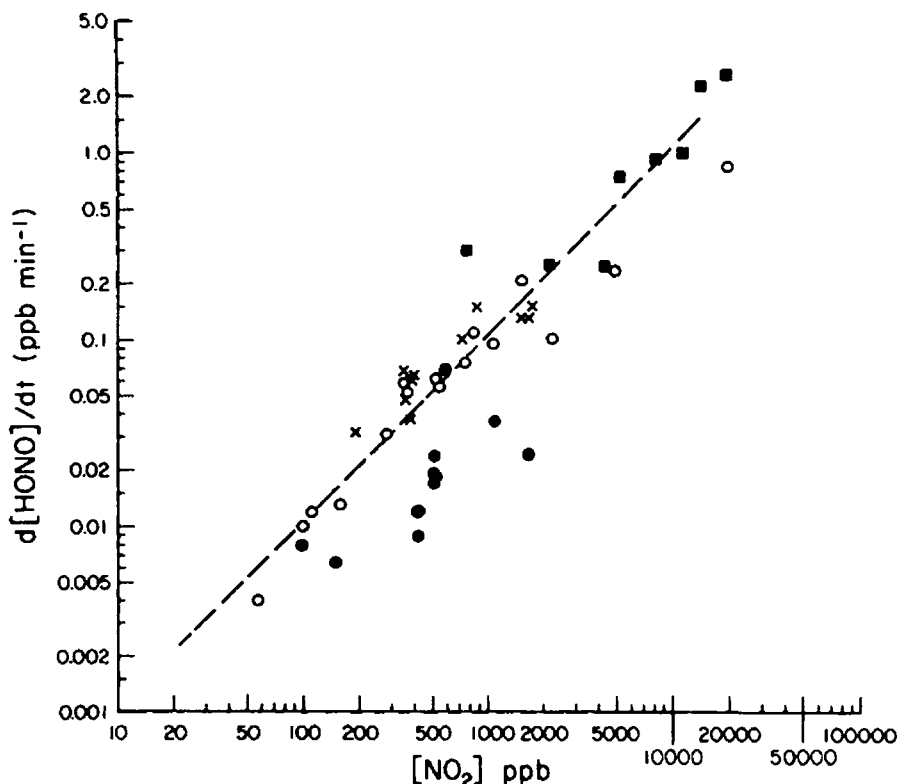

Figure 2. Plot of the HONO formation rate $dt[HONO]/dt$ against the NO_2 concentration for the SAPRC and NIES chambers at ca.50% relative humidity. (X) SAPRC 5800-L evacuable chamber, T = 305 K; (O) SAPRC 5800-L evacuable chamber, T = 297 K; (●) SAPRC 4300-L all-Teflon chamber, T = 297 K; (■) NIES 6065-L evacuable chamber, T = 303 K. The dashed line is the best-fit line with unit slope through the data for the SAPRC 5800-L evacuable chamber.
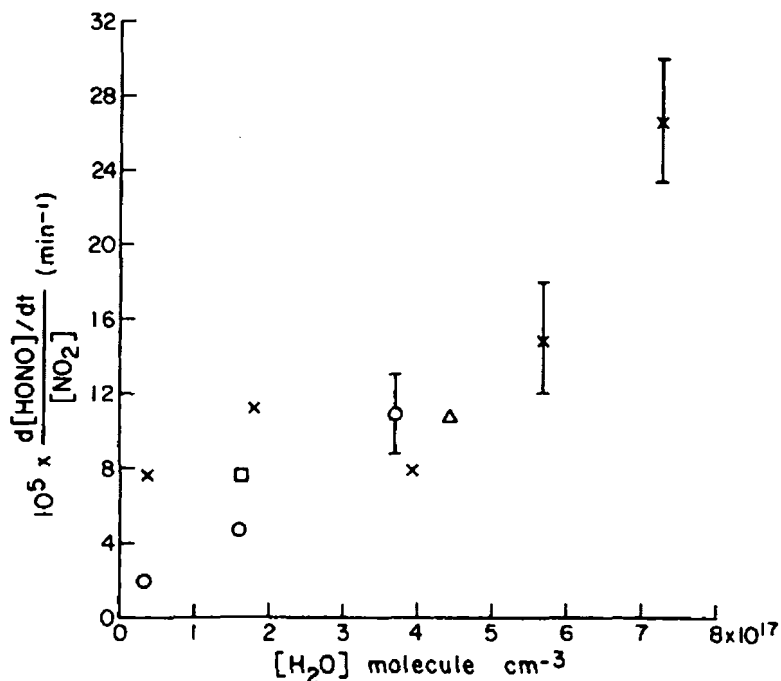
Figure 3. Plot of the HONO formation rate, normalized by the NO_2 concentration, for the SAPRC 5800-L evacuable chamber against the H_2O concentration at the various temperatures studied. ($\triangle$) 323 K, ($\times$) 305 K, (O) 297 K, ($\square$) 283 K.

of temperature on the HONO formation rate. However, it is apparent that the water concentration has a larger effect on the HONO formation rate than does the temperature, at least when varied within the range employed in these experiments.

One experiment (EC-784) was carried out specifically to detect gas phase nitric acid. Using long path Fourier transform infrared (FTIR) spectroscopy, no evidence for gas phase HNO_3 was obtained during this run (the detection limit for HNO_3 was ca.40 ppb). Since the maximum HONO concentration observed by FTIR spectroscopy in this experiment was 387 ppb, the gas phase HNO_3 concentration was at least a factor of 10 lower than that of HONO.

All-Teflon Chamber Studies

The initial reactant concentrations and the data obtained in the 4300-L Teflon chamber are given in Table II. The initial HONO formation rates are also plotted against the initial NO_2 concentrations in Figure 2 to allow comparison with the results from the 5800-L evacuable chamber. The results were similar to those in the evacuable chamber in that continuous HONO formation from NO_2 was observed in all cases. However, the HONO formation rates obtained in this

TABLE II. Rates of dark HONO formation from NO_x/H_2O/air mixtures in the all-Teflon chamber.

ATC Run Number	Initial $[NO_2]$ (ppb)	Temp (°K)	RH (%)	Initial			Final		
				$d[HONO]/dt$ (ppb min^{-1})	$-d[NO_2]/dt$ (ppb min^{-1})	$\dfrac{d[HONO]/dt}{-d[NO_2]/dt}$	t (min)	$\Delta[NO_2]$ (ppb)	$\dfrac{\Delta[HONO]}{\Delta[NO_2]}$
4	1100	297	50	0.036 ± 0.007	0.122 ± 0.02	0.29	400	49	0.30
6	537	297	50	0.018 ± 0.0012	0.084 ± 0.02	0.21	1560	78	0.33
7	515	297	50	0.0235 ± 0.0015	-	-	1250	89	0.39
8	513	296	50	0.017 ± 0.001	0.11 ± 0.015	0.20	1350	80	0.30
9	99	296	50	0.0079 ± 0.002			-	-	-
10	506	296	50	0.019 ± 0.002	0.065 ± 0.01	0.29	1150	66	0.12
13	420	297	50	0.0087 ± 0.001	0.085 ± 0.01	0.10	1500	73	0.16
14	425	297	50	0.012 ± 0.002	-	-	1300	50	0.30
15	1680	298	50	0.024 ± 0.002	-		1400	200	0.17
16	150	298	50	0.0064 ± 0.0004	-		3000	53	0.36

chamber showed substantially more scatter than those in the 5800-L evacuable chamber, and generally indicated lower HONO formation rates for a given NO_2 concentration. In addition, Table II shows that, in contrast to the 5800-L evacuable chamber, the initial stoichiometry $(\Delta[HONO]/-\Delta[NO_2])_{init}$ was less than 0.5, with values as low as 0.1 (ATC-13), and that these stoichiometry values showed a significant degree of scatter.

Discussion

HONO Formation in Environmental Chambers

The initial HONO formation rates observed in the SAPRC evacuable and Teflon chambers at 50% RH and 297–305 K, together with those reported by Sakamaki, Hatakeyama, and Akimoto [14] at much higher initial NO_2 concentrations for the 6065-L evacuable chamber at the National Institute for Environmental Studies (NIES) in Japan at ca.50% RH and 303 K, are shown in Figure 2. It can be seen from this figure that the present data are qualitatively and quantitatively similar to those of Sakamaki, Hatakeyama, and Akimoto [14]. This suggests that the mechanism, at least for the initial portion of the reaction, does not change as the reactant concentrations are reduced below those employed by Sakamaki, Hatakeyama, and Akimoto [14] to levels more representative of atmospheric conditions. In particular, the data for a given chamber fall reasonably close to a line of slope $\{d \ln(d[HONO]/dt)/d[NO_2]\}_{init} = 1.0$, indicating that the initial HONO formation rate is approximately first order with respect to the initial NO_2 concentration throughout this concentration range.

The data for the 4300-L all-Teflon reaction chamber fall somewhat below the line drawn through our data points obtained in the SAPRC 5800-L evacuable chamber (dashed line in Fig. 2), while the data for the NIES evacuable chamber [14] fit well on this line. Thus, as expected, the HONO formation rate from NO_2 appears to be chamber dependent, with the SAPRC all-Teflon chamber being less reactive than both the SAPRC and the NIES evacuable chambers. The chamber characteristics and the averages of the observed initial first-order rates of HONO formation $\{(d[HONO]/dt)/[NO_2]\}_{init}$ and of NO_2 consumption $\{(-d[NO_2]/dt)/[NO_2]\}_{init}$ for each of these three chambers are summarized in Table III.

The results of the present study support previous conclusions [7,14,15] that HONO formation does not occur to any significant extent from the reaction

$$(3) \qquad NO + NO_2 + H_2O \rightarrow 2\,HONO$$

In particular, our data yield an upper limit for this reaction of $k_3 < 6 \times 10^{-38}$ cm^6 molecule^{-2} s^{-1}. This is totally consistent with the value

TABLE III. Comparison of chamber characteristics and average apparent first-order rate constants for HONO formation and NO_2 consumption in three environmental chambers at ca. 50% RH and ca. 300 K.

Chamber	NIES Evacuable[a]	SAPRC Evacuable	SAPRC All-Teflon
Volume (ℓ)	6065	5800	4300
Surface/volume (m^{-1})	3.6	3.4	3.4
Surface[b]	91% PFA[c] Teflon coated stainless steel 9% quartz	~82% FEP Teflon coated aluminum ~18% quartz	100% 2-mil thick FEP Teflon film
$\dfrac{d[HONO]/dt}{[NO_2]}$ (10^{-4} min^{-1})[e]	1.3 ± 0.4[d]	1.2 ± 0.4	0.4 ± 0.2
$\dfrac{-d[NO_2]/dt}{[NO_2]}$ (10^{-4} min^{-1})[e]	4.4 ± 1.1[d]	2.8 ± 1.2	1.6 ± 0.5
$\dfrac{d[HONO]/dt}{-d[NO_2]/dt}$[e]	0.30 ± 0.10[d]	0.44 ± 0.06	0.21 ± 0.08

[a] As described by Sakamaki, Hatakeyama, and Akimoto [14].
[b] Excluding IR or DOAS multi-reflection optics.
[c] PFA = tetrafluoroethylene-perfluoroalkyl vinyl ether copolymer.
[d] Average of data for runs 7–13 and 15–17 in Table II of [14].
[e] Initial values.

of $k_3 < 9 \times 10^{-39}$ cm^6 molecule^{-2} s^{-1} derived by Sakamaki, Hatakeyama, and Akimoto [14] for the NIES evacuable chamber, and with the value $k_3 \leqslant 4.4 \times 10^{-40}$ cm^6 molecule^{-2} s^{-1} derived by Kaiser and Wu [15] for a 0.75-L Pyrex reaction vessel. It should be noted that our upper limit of $k_3 < 6 \times 10^{-38}$ cm^6 molecule^{-2} s^{-1} corresponds to an upper limit of $k_{-3} < 9 \times 10^{-19}$ cm^3 molecule^{-1} s^{-1} for the reverse reaction,

(−3) $HONO + HONO \rightarrow NO + NO_2 + H_2O$

based on the equilibrium constant $k_3/k_{-3} = 7.0 \times 10^{-20}$ cm^3 molecule^{-1} at 298 K [20]. The gas phase reaction (−3) is this also negligible under our experimental conditions (see below).

Thus the present data indicate that reaction of NO_2 with water vapor is the source of HONO in these chambers, in agreement with the conclusion of Sakamaki, Hatakeyama, and Akimoto [14]. Although the overall reaction may occur via

(4) $2 NO_2 + H_2O \rightarrow HONO + HNO_3$
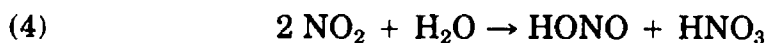
the rate determining step is first-, and not second-, order in NO_2. Furthermore, HNO_3 was not observed in the gas phase in either the

present work or by Sakamaki, Hatakeyama, and Akimoto [14]. However, reaction (4) is consistent with the lack of a dependence of the HONO formation rate on the NO concentration, and also with the observation that the HONO formation rate was equal or less than half of the NO_2 consumption rate.
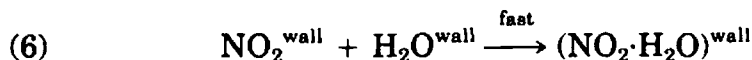
The reverse reaction

$$(-4) \qquad HNO_3 + HONO \rightarrow 2\,NO_2 + H_2O$$
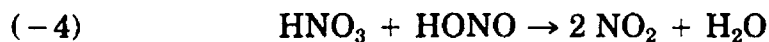
has been studied in the gas phase by Kaiser and Wu [21] and Streit et al. [22] who obtained a rate constant of $k_{-4} \simeq 1 \times 10^{-17}$ cm^3 molecule^{-1} s^{-1} at room temperature. Kaiser and Wu [21] observed that this reaction was sensitive to surface conditions, and hence this rate constant must be considered to be an upper limit. Using this upper limit value for k_{-4} and the equilibrium constant $k_4/k_{-4} = 3.9 \times 10^{-21}$ cm^3 molecule^{-1} [20], a value of $k_4 \leqslant 4 \times 10^{-38}$ cm^6 molecule^{-2} s^{-1} is obtained for the homogeneous gas phase reaction. This upper limit value for k_4 leads to HONO formation rates much lower than those observed experimentally when $[NO_2] < 1$ ppm (see Tables I and II) and much higher than those observed when $[NO_2] \geqslant 5$ ppm (see Table I and [14]).

These conditions, together with the observed first-order dependence of HONO formation on the NO_2 concentration, indicate that if reaction (4) is the source of HONO in these chambers it must occur heterogeneously. Indeed, from the data of Sakamaki, Hatakeyama, and Akimoto [14] an upper limit of $k_4 \leqslant 1.8 \times 10^{-38}$ cm^6 molecule^{-2} s^{-1} (lower than that derived above) can be obtained for the homogeneous third-order rate constant. This value then makes the homogeneous reaction (4) totally negligible in our experiments.
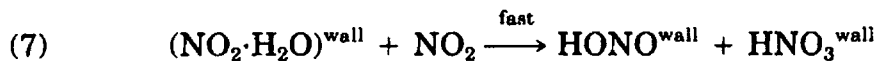
There are at least three possible mechanisms which are consistent with our experimental data. In the first two, reaction (5) is the rate determining step, followed by either reaction (4) or reactions (6) and (7)

$$(5) \qquad NO_2{}^{gas} \xrightarrow{\text{slow}} NO_2{}^{wall}$$

$$(4) \qquad 2\,NO_2{}^{wall} + H_2O^{wall} \xrightarrow{\text{fast}} HONO^{wall} + HNO_3{}^{wall}$$

or

$$(6) \qquad NO_2{}^{wall} + H_2O^{wall} \xrightarrow{\text{fast}} (NO_2 \cdot H_2O)^{wall}$$

and

$$(7) \qquad (NO_2 \cdot H_2O)^{wall} + NO_2 \xrightarrow{\text{fast}} HONO^{wall} + HNO_3{}^{wall}$$

In these cases, adsorption of NO_2 must be rate determining to explain
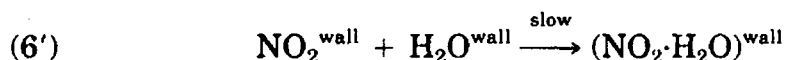
the first-order dependence on NO_2, and this adsorption onto the wall must also depend on the water vapor concentration (Fig. 3).

A third possible reaction involves rapid adsorption of NO_2 onto the wall,

$$(5') \qquad NO_2{}^{gas} \xrightarrow{\text{fast}} NO_2{}^{wall}$$

followed by the slow formation of a surface $(NO_2 \cdot H_2O)$ complex [reaction $(6')$]

$$(6') \qquad NO_2{}^{wall} + H_2O{}^{wall} \xrightarrow{\text{slow}} (NO_2 \cdot H_2O)^{wall}$$

The subsequent rapid reaction (7) then leads to the final products. In all cases the HONO formed on the wall will be desorbed into the gas phase.

$$(8) \qquad HONO^{wall} \to HONO^{gas}$$

The above schemes are almost certainly oversimplifications of this system. However, until additional data are available concerning the behavior of the various nitrogen oxides and oxyacids on surfaces, further speculation concerning the details of these reactions is unwarranted.

Although HNO_3 is expected to be formed as a co-product along with HONO in the hydrolysis of NO_2, HNO_3 was not observed in the gas phase either in our study or in that of Sakamaki, Hatakeyama, and Akimoto [14]. Instead, an apparent loss of gas phase nitrogen, at rates approximately corresponding to the expected rates of HNO_3 formation, has been observed. Thus it appears that, unlike HONO, if HNO_3 is formed in a surface reaction such as reactions (4) or (7), it remains on the surface, being desorbed only slowly, if at all. This conclusion is consistent with recent data from our laboratories [23] that gas phase HNO_3 decays to the walls in the evacuable chamber with lifetimes of ca.13 h at ca.2% RH and ca.1.6 h at ca.50% RH. Furthermore, it is possible that HNO_3 adsorbed on the wall may oxidize adsorbed organics leading to the formation of NO, as observed in both our study and that of Sakamaki, Hatakeyama, and Akimoto [14].

As noted earlier, after extended periods of time the rates of HONO formation decreased (see, for example Fig. 1) and the formation of NO (presumably a secondary product) was observed. Additionally, in most runs the disappearance rate of NO_2 also decreased with time, though this decrease was generally relatively less than the decrease in the HONO formation rate. The final yields of HONO, NO, and lost nitrogen for the evacuable chamber experiments in which NO was measured are summarized in Table I. It can be seen that in all cases ca.40–60% of the NO_2 reacted is lost from the gas phase and, for the

runs performed for the longest duration, the final yield of NO approaches the final yields of HONO.

While the formation of NO and the reduced rate of HONO formation late in these experiments could be caused by the decomposition of HONO or by reaction of HONO with NO_2

$$(-3) \qquad 2\ HONO \rightarrow NO + NO_2 + H_2O$$

$$(9) \qquad NO_2 + HONO \rightarrow HNO_3 + NO$$
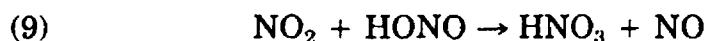
the upper limits obtained in this work for k_{-3} and by Streit et al. [22] for k_{-9} (combined with the equilibrium constant k_9/k_{-9} [20]) allows these homogeneous gas phase reactions to be ruled out as the source of NO.

Implications Concerning Chamber Radical Sources

As discussed in the Introduction, the dark formation of HONO from NO_2, whose importance in environmental chambers had been proposed earlier [6,7] and has now been established by this study and that of Sakamaki, Hatakeyama, and Akimoto [14], will contribute, at least in part, to the excess rate of radical initiation characteristic of NO_x-air and NO_x-organic-air irradiations in environmental chambers. Thus in a recent detailed investigation of this problem [6,7], carried out in four different environmental chambers (including the evacuable chamber used in this study and an all-Teflon chamber similar to the one used here), it was concluded that "unknown" sources of OH radicals were present in all of the chambers studied and that two distinct radical sources were necessary to explain the data: (1) the photolysis of initially present HONO, whose importance increased with increasing NO_2/NO concentration ratios, but which was a minor contributor to the overall radical flux after 30–60 min of irradiation, and (2) a constant (for those NO_x-air irradiations) radical source which dominated beyond the first ca.60 min of irradiation. After the first ca.30–60 min of irradiation, the radical input rates were observed to be independent of the NO concentration, to increase with increasing temperature, humidity and NO_2 concentration, to be proportional to the light intensity, and to be dependent on the chamber employed [7].

The present results show that in environmental chambers significant amounts of HONO will be present at the commencement of irradiation, since environmental chamber experiments generally involve some elapsed time between the injection of NO_2 and the beginning of the irradiation. The photolysis of this initially present HONO then explains the rapidly decaying radical source which is observed in such experiments.

However, the rates of HONO formation from the dark reaction of NO_2 with H_2O in the evacuable chamber in this study are a factor of ca.10 smaller than the continuous radical input rates determined for this chamber [7]. Hence, the continuous production of HONO from NO_2 and the subsequent photolysis of HONO can only explain ca.10% of the unknown radical source after ca.60 min of irradiation. However, it is interesting that the production of HONO in the dark has a very similar behavior to this unknown continuous radical source. Thus both increase linearly with the NO_2 levels, neither are affected by changes in the NO concentration, and both increase with the water vapor concentration. These facts strongly suggest that the interaction between NO_2 and H_2O and the chamber walls, which are responsible for dark HONO formation, could also be involved in the production of radicals during the irradiations. However, the details of this process remain elusive at present.

HONO Formation in Polluted Atmosphere

The fact that HONO is observed to continuously increase at night in urban atmospheres (up to ca.8 ppb near downtown Los Angeles) when NO_2 and (frequently) NO levels are relatively constant [4,8] is strongly suggestive that HONO is formed in the atmosphere through one or more chemical reactions. However, in view of our direct measurements of HONO in auto exhaust [10] it is also possible that the observed nighttime increase in HONO may be due, at least in part, to direct emissions.

Recently Stockwell and Calvert [9] have postulated that HONO is formed in nighttime atmospheres from the reaction of HO_2 radicals with NO_2 [reaction (10)].

(10) $\qquad HO_2 + NO_2 \rightarrow HONO + O_2$
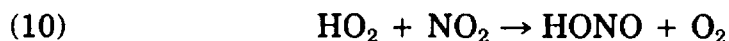
Although there are a variety of sources of HO_2 radicals at night, Stockwell and Calvert [9] concluded, based upon a chemical computer modeling study and, in the absence of experimental data, using an HCHO concentration of 20 ppb, that the major source of HO_2 radicals arises from reaction (11) followed by reaction (12), which is rapid in one atmosphere of air.

(11) $\qquad NO_3 + HCHO \rightarrow HNO_3 + HCO$

(12) $\qquad HCO + O_2 \rightarrow HO_2 + CO$
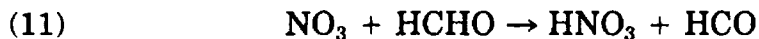
In the absence of experimental data, the rate constant k_{11} was assumed [9] to be equal to that for the reaction of NO_3 radicals with CH_3CHO $(1.4 \times 10^{-15}$ cm^3 molecule^{-1} s^{-1} at 300 K [24]). While the assumed

HCHO level of 20 ppb is consistent with late evening measurements reported by Grosjean [25], recent measurements in this laboratory [26] have shown that $k_{11} = 3.2 \times 10^{-16}$ cm^3 molecule^{-1} s^{-1}, a factor of 4 lower than that assumed by Stockwell and Calvert [9]. Thus the reaction sequence (10)–(12) seems unlikely to be a significant formation route to nighttime HONO under typical ambient conditions.

Based on the available data, it appears that a combination of direct HONO emissions [10] and heterogeneous formation via the hydrolysis of NO$_2$ are responsible for the formation of HONO at night. Indeed, the HONO formation rate observed in the SAPRC 5800-L evacuable chamber at ca.300 K and ca.50% RH leads to the formation of ca.5 ppb of HONO over an 8-h time period. While perhaps fortuitous, since in general one would expect rates of heterogeneous processes to vary greatly with different surfaces, this level falls within the range of maximum HONO levels of ca.2–8 ppb we have observed in urban atmospheres by DOAS [4,8], suggesting that such a heterogeneous process may be the mechanism predominantly responsible for nighttime HONO formation.

Acknowledgment

Bibliography

[1] W. R. Stockwell and J. G. Calvert, *J. Photochem.*, 8, 193 (1978).

[2] K. L. Demerjian, J. A. Kerr, and J. G. Calvert, *Adv. Environ. Sci. Technol.*, 4, 1 (1974).

[3] B. J. Finlayson-Pitts and J. N. Pitts, Jr., *Adv. Environ. Sci. Technol.*, 7, 75 (1977).

[4] G. W. Harris, W. P. L. Carter, A. M. Winer, J. N. Pitts, Jr., U. Platt, and D. Perner, *Environ. Sci. Technol.*, 16, 414 (1982).

[5] R. Atkinson and A. C. Lloyd, *J. Phys. Chem. Ref. Data*, in press.

[6] W. P. L. Carter, R. Atkinson, A. M. Winer, and J. N. Pitts, Jr., *Int. J. Chem. Kinet.*, 13, 735 (1981).

[7] W. P. L. Carter, R. Atkinson, A. M. Winer, and J. N. Pitts, Jr., *Int. J. Chem. Kinet.*, 14, 1071 (1982).

[8] U. Platt, D. Perner, G. W. Harris, A. M. Winer, and J. N. Pitts, Jr., *Nature (London)*, 285, 312 (1980).

[9] W. R. Stockwell and J. G. Calvert, *J. Geophys. Res.*, 88, 6673 (1983).

[10] J. N. Pitts, Jr., H. W. Biermann, E. C. Tuazon, and A. M. Winer, *Atmos. Environ.*, in press.

[11] W. P. L. Carter, A. C. Lloyd, J. L. Sprung, and J. N. Pitts, Jr., *Int. J. Chem. Kinet.*, **11**, 45 (1979).

[12] W. H. Chan, R. J. Nordstrom, J. G. Calvert, and J. H. Shaw, *Environ. Sci. Technol.*, **10**, 674 (1976).

[13] W. H. Chan, R. J. Nordstrom, J. G. Calvert, and J. H. Shaw, *Chem. Phys. Lett.*, **37**, 441 (1976).

[14] F. Sakamaki, S. Hatakeyama, and H. Akimoto, *Int. J. Chem. Kinet.*, **15**, 1013 (1983).

[15] E. W. Kaiser and C. H. Wu, *J. Phys. Chem.*, **81**, 1701 (1977).

[16] C. England and W. H. Corcoran, *Ind. Eng. Chem. Fundam.*, **13**, 373 (1974).

[17] Y.-N. Lee and S. E. Schwartz, *J. Phys. Chem.*, **85**, 840 (1981).

[18] A. M. Winer, R. A. Graham, G. J. Doyle, P. J. Bekowies, J. M. McAfee, and J. N. Pitts, Jr., *Adv. Environ. Sci. Technol.*, **10**, 461 (1980).

[19] G. J. Doyle, P. J. Bekowies, A. M. Winer, and J. N. Pitts, Jr., *Environ. Sci. Technol.*, **11**, 45 (1977).

[20] S. E. Schwartz and W. H. White, *Adv. Environ. Sci. Eng.*, **4**, 1 (1981).

[21] E. W. Kaiser and C. H. Wu, *J. Phys. Chem.*, **81**, 187 (1977).

[22] G. E. Streit, J. S. Wells, F. C. Fehsenfeld, and C. J. Howard, *J. Chem. Phys.*, **70**, 3439 (1979).

[23] E. C. Tuazon, R. Atkinson, C. N. Plum, A. M. Winer, and J. N. Pitts, Jr., *Geophys. Res. Lett.*, **10**, 953 (1983).

[24] E. D. Morris, Jr., and H. Niki, *J. Phys. Chem.*, **78**, 1337 (1974).

[25] D. Grosjean, *Environ. Sci. Technol.*, **16**, 254 (1982).

[26] R. Atkinson, C. N. Plum, W. P. L. Carter, A. M. Winer, and J. N. Pitts, Jr., *J. Phys. Chem.*, **88**, 1210 (1984).